Am J Physiol Heart Circ Physiol 302: H885–H892, 2012.
First published December 6, 2011; doi:10.1152/ajpheart.00985.2011.

Left ventricular torsion, energetics, and diastolic function in normal human aging

Kieren G. Hollingsworth,[1,2] Andrew M. Blamire,[1,2] Bernard D. Keavney,[3] and Guy A. MacGowan[3,4]

[1]*Newcastle Magnetic Resonance Centre, Institute of Cellular Medicine, Newcastle University, Newcastle upon Tyne;* [2]*Institute of Cellular Medicine, Medical School, Newcastle University, Newcastle upon Tyne;* [3]*Institute of Genetic Medicine, Newcastle University, International Centre for Life, Newcastle upon Tyne; and* [4]*Department of Cardiology, Freeman Hospital, Newcastle upon Tyne, United Kingdom*

Submitted 14 October 2011; accepted in final form 14 December 2011

Hollingsworth KG, Blamire AM, Keavney BD, MacGowan GA. Left ventricular torsion, energetics, and diastolic function in normal human aging. *Am J Physiol Heart Circ Physiol* 302: H885–H892, 2012. First published December 6, 2011; doi:10.1152/ajpheart.00985.2011.—This study determined, for the first time, whether the effects of normal aging on systolic and diastolic left ventricular function in subjects without cardiovascular disease are related to underlying energetic defects. Cardiac magnetic resonance imaging with tissue tagging and ^{31}P spectroscopy was used to determine global structure, function, myocardial strains, and the phosphocreatine-to-ATP ratio (PCr/ATP) in 49 healthy subjects aged 20–69 yr. The three major abnormalities that developed with increasing age were the early filling percentage (EFP, the left ventricular volume increase from end systole to mid-diastole divided by stroke volume × 100), which decreased with age, indicating impaired early diastolic filling ($r = -0.72$, $P < 0.0001$), the torsion-to-shortening ratio (TSR, measure of subepicardial torsion exerting mechanical advantage over subendocardial shortening), which increased with age indicating relative subendocardial dysfunction ($r = 0.44$, $P < 0.02$), and the PCr/ATP (decreased with increasing age, $r = -0.52$, $P < 0.003$). EFP and TSR were strongly correlated ($r = -0.63$, $P < 0.0001$), although they were not related to PCr/ATP [EFP vs. PCr/ATP: $r = 0.34$, not significant (NS) and TSR vs. PCr/ATP: $r = -0.3$, P = NS]. In normal aging, changes in EFP and TSR likely share the same pathophysiology, although it is unlikely that energetics have a major role in the functional effects of aging.

aging; normal; left ventricular function; energetics

CARDIOVASCULAR FUNCTION CHANGES with age. From the third decade onward, there is an increase in vascular stiffening in both men and women (34). This is thought to have significant effects on cardiac function, and in particular left ventricular (LV) diastolic function (4). The LV early diastolic filling rate progressively slows after the age of 20 years, so that by 80 years the rate is reduced by almost 50% (31). Global systolic function in terms of ejection fraction or stroke volume does not appear to change with age in the absence of specific pathological processes affecting the myocardium (18).

Despite the apparent lack of changes in global systolic function during healthy aging, studies examining intramyocardial strains have shown significant effects of aging (19, 25). Magnetic resonance (MR) tissue tagging is a noninvasive labeling technique using a presaturation pulse (37) to create signal voids that, when placed on the image at end diastole, can persist throughout the cardiac cycle. Myocardial shortening in circumferential, radial, and longitudinal planes, systolic torsion, and diastolic recoil can all be assessed. Based on the fiber architecture of the left ventricle with left-handed subepicardial and right-handed subendocardial fiber orientations, the left ventricle exhibits a characteristic systolic rotational deformation termed torsion (6). Torsion occurs as a consequence of the greater radius of the subepicardial fibers exerting a mechanical advantage over subendocardial fibers (27). This mechanical advantage has been expressed in terms of a ratio of subepicardial torsion to subendocardial circumferential strain (1, 19) referred to as the torsion-to-shortening ratio (TSR). This ratio is increased during normal aging and may represent relative subendocardial dysfunction, perhaps as a consequence of subendocardial fibrosis.

Cardiac energetics also change with age. The creatine kinase enzyme system functions both as an important energy buffer and as an energy shuttle between the mitochondria and myofibrils. When the heart starts to fail, levels of phosphocreatine (PCr) fall as energy utilization exceeds supply. ATP levels are also reduced, although to a much lesser extent (22). The ratio PCr/ATP, which can be measured noninvasively by phosphorus magnetic resonance spectroscopy (^{31}P-MRS), is reduced in heart failure, and this ratio is a predictor of mortality (23). In a mouse model of pressure-overload hypertrophy, early changes in PCr/ATP correlated with increases in LV end-diastolic volume that developed over the subsequent 3 wk, suggesting that altered high-energy phosphate metabolism is an early feature of contractile dysfunction (21). Schocke et al. (29) have shown with MRS that with increasing age there are significant decreases in the PCr/ATP ratio.

Thus, there is evidence that there are changes in LV systolic strains, global diastolic function, and energetics with age. We do not know, however, if these changes share the same pathophysiology, but we can study all these with MR imaging and spectroscopy. Potentially energetic abnormalities might contribute to functional defects (20). The purpose of this study was to investigate the temporal development of age-related changes in ventricular function and energetics in a single cross-sectional patient cohort and test the hypothesis that systolic and diastolic changes are significantly related to changes in cardiac energetics.

METHODS

Subjects. Forty-nine subjects (25 males, 24 females) aged between 20 and 69 yr were recruited into three discrete age bands, with approximately equal numbers of men and women in each: 20–40, 40–60, and over 60 years old. This allowed for comparison of

Address for reprint requests and other correspondence: K. G. Hollingsworth, Newcastle Magnetic Resonance Centre, Institute of Cellular Medicine, Campus for Ageing and Vitality, Newcastle Univ., NE4 5PL (e-mail: k.g.hollingsworth@ncl.ac.uk).

changes among the three age groups and ensured a consistent distribution of subjects throughout the whole study group. Subjects were matched as closely as possible for body mass index and weight.

All subjects had no previous history of cardiac disease and were screened with a 12-lead electrocardiogram (ECG) and blood pressure measurements. Subjects with hypertension (systolic blood pressure >150 mmHg and/or diastolic blood pressure >90 mmHg) were excluded from the study. Blood pressure measurements were recorded before the subjects entered the scanner. The subjects underwent an MR protocol of MR cine imaging, cardiac tagging, and phosphorus cardiac spectroscopy, performed at a single session. Local ethical approval for the study was sought from the Newcastle Research Ethics Committee and was approved: individual informed consent was obtained from the participants and the study complies with the Declaration of Helsinki.

Cardiac MR cine imaging. Cardiac examinations were performed using a 3T Philips Intera Achieva scanner (Best, NL). A dedicated six-channel cardiac coil (Philips) was used with the subjects in a supine position and ECG gating. Short-axis balanced steady-state free precession images were acquired covering the left ventricle [field of view (FOV) = 350 mm, repetition time (TR)/echo time (TE) = 3.7/1.9 ms, acceleration factor 17, flip angle 40°, slice thickness 8 mm, 0 mm gap, 14 slices, 25 phases, resolution 1.37 mm]. Image analysis was performed using the cardiac analysis package of the ViewForum workstation (Philips). Manual tracing of the epicardial and endocardial borders was performed on the short-axis slices at end systole and end diastole. Details of our algorithm for contour selection and calculating LV mass and systolic and diastolic parameters have been previously published (14). The eccentricity ratio of the LV mass to the end-diastolic volume was calculated, since this parameter is a measure of concentric remodeling. Preload, afterload, contractility, and ventricular-arterial coupling were calculated. Preload was determined by the end-diastolic volume, afterload by arterial elastance [E_a = end-systolic pressure (systolic blood pressure × 0.9)/stroke volume (normalized to body surface area)], contractility by end-systolic elastance [(E_{es}) = end-systolic pressure/end-systolic volume (normalized to body surface area)], and ventricular-arterial coupling by the ratio of E_{es}/E_a.

Cardiac spectroscopy. Cardiac high-energy phosphate metabolism was assessed using ^{31}P-MRS. Data were collected using the same 3T Intera Achieva scanner (Philips) with a 10-cm-diameter ^{31}P surface coil (Pulseteq, UK) for transmission/reception of signal. Subjects were placed in a prone position and moved into the magnet so their heart was at magnet isocenter. Localizing images were collected using the in-built body coil to confirm location of the heart. Shimming was performed using a cardiac-triggered, breath-held field map (28). A slice-selective, cardiac-gated one-dimensional chemical shift imaging sequence was used with a 7-cm slice-selective pulse applied foot to head to eliminate contamination from the liver, with spatial presaturation of lateral skeletal muscle to avoid spectral contamination. Sixteen coronal phase-encoding steps were used, yielding spectra from 10-mm slices (TR = heart rate, 192 averages at the center of k-space with cosine-squared acquisition weighting, ~20 min acquisition time). Spectral locations were overlaid onto an anatomical image, and the first spectrum arising entirely beyond the chest wall was selected. Quantification of PCr, the γ resonance of ATP, and 2,3-diphosphoglycerate (DPG) was performed using the AMARES time domain fit routine in the jMRUI processing software. After fitting, the ATP peak area was corrected for blood contamination by one-sixth of the amplitude of the combined 2,3-DPG peak (9), and the PCr/ATP ratios were calculated and corrected for saturation, with T_1 relaxation time values of cardiac PCr and ATP taken from the literature (33). Flip angle correction was made using a gadolinium-doped 20 mM phenyl phosphonic acid phantom at the center of the coil and a calibration dataset (7, 11).

Cardiac tagging. Tagged short-axis images were acquired. Cardiac tagging works by applying radiofrequency pulses to cancel MR signal from the myocardium in diastole in a rectangular grid pattern and tracking the deformation of these tags through the rest of the cardiac cycle (Fig. 1*A*). A turbo field echo sequence with an acceleration factor of nine was used (TR/TE/flip angle/NEX = 4.9/3.1/10°/1, SENSE factor 2, FOV 350 × 350 mm, voxel size 1.37 × 1.37 mm, tag spacing of 7 mm). Two adjacent short-axis slices of 10 mm thickness were acquired at midventricle with a 2-mm gap. The Cardiac Image Modelling package (University of Auckland) was used to analyze the tagging data by aligning a mesh on the tags between the endo- and epicardial contours. Circumferential strain and the rotation of the two planes were calculated throughout the cardiac cycle. Circumferential strain is quoted for both the whole myocardial wall and the endocardial third of the wall thickness. The epicardial torsion between the two planes (taken as the circumferential-longitudinal shear angle defined on the epicardial surface) was calculated (6) (Fig. 1*B*).

In the healthy heart, torsion occurs such that there is homogeneity of fiber shortening across the myocardial wall and is a marker of the

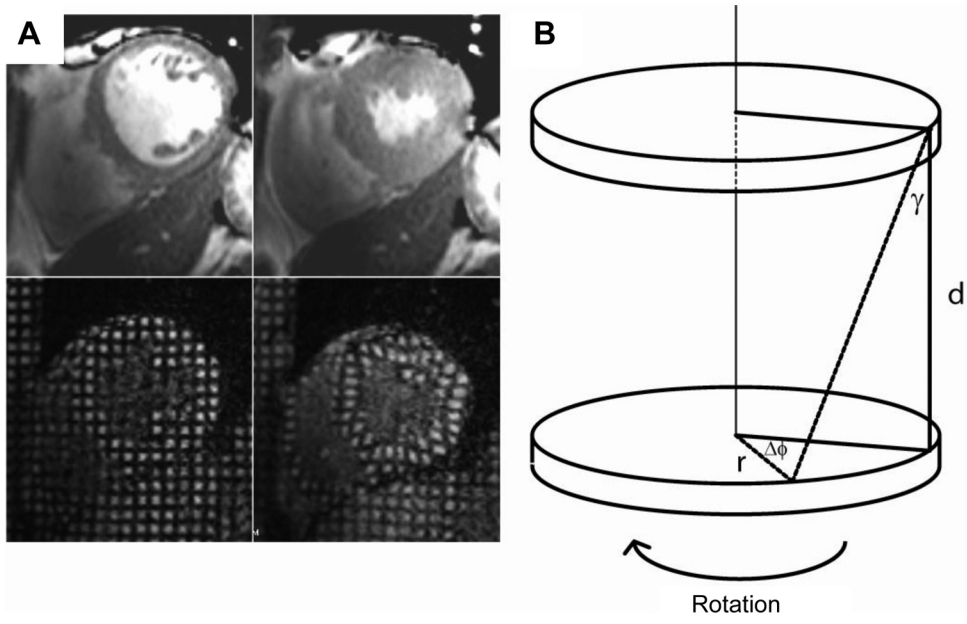

Fig. 1. *A*: cardiac cine imaging (*top*) and cardiac tagging (*bottom*) at diastole (*left*) and systole (*right*), showing how a rectangular grid of nulled signal applied at diastole remains with the tissue through the cardiac cycle, allowing calculation of strain and torsion. *B*: tagging in two parallel sections allows the calculation of the torsion (the longitudinal-circumferential shear angle γ) between two short-axis planes a distance *d* apart with radius *r* where one short-axis plane rotates through Δϕ relative to the other. $\gamma = \tan^{-1}\{[2r \sin(\Delta\phi/2)]/d\}$.

dominance of epicardial fibers over endocardial fibers as a consequence of the greater radius in the epicardium. This can be quantified by a ratio of the peak torsion (in radians), defined as the shear angle between two planes on the epicardial surface (19), and the peak circumferential strain in the endocardial third of the myocardium and is referred to as the TSR (19, 35). This ratio has been shown to be near constant among healthy subjects of the same age and to increase with both healthy aging and disease. The recoil of torsion in diastole occurs rapidly in early diastole and has been shown to correlate closely with the time constant of isovolumic relaxation derived from the LV pressure waveform (10). This was expressed as maximum torsion gradient in diastole (deg/ms, defined as the maximum slope of the torsion curve in diastole), the torsion recoil rate (which is normalized for peak torsion, %/ms), and the residual torsion at 150% of the end-systolic time.

Longitudinal shortening was determined from cine-magnetic resonance imaging (MRI) in the four-chamber view by determining the perpendicular distance from the plane of the mitral valve to the apex in systole and diastole. The myocardial wall thickness at systole and diastole was determined at the same level as the cardiac tagging, and radial thickening was calculated.

Statistical analysis. Analysis was performed blinded to age or identity of research subjects. Statistical testing was performed using SPSS version 17. Data are presented as means and SD. Comparisons in means were drawn between groups using ANOVA with post hoc Bonferroni correction for multiple comparisons. Linear correlations were executed as a two-tailed test using the Pearson correlation method with post hoc Bonferroni correction for multiple comparisons. Statistical significance level was taken to be $P < 0.05$.

RESULTS

Global cardiac systolic function and structure. There were no significant changes in LV mass, LV index, ejection fraction, resting heart rate, cardiac output, or stroke volume between the groups (Table 1). There was a significant difference between young and middle-aged subjects for end-diastolic and end-systolic volume (Table 1), with middle-aged subjects having lower end-diastolic and end-systolic volumes than either younger or older subjects. As a consequence, the eccentricity ratio of the middle-aged group was also significantly higher than the young or older groups. E_a was significantly elevated from middle age onward, ventricular elastance was significantly elevated at middle age compared with younger subjects, and there were no significant changes in ventricular-arterial coupling.

Diastolic function and cardiac energetics. Diastolic function was progressively reduced across the age groups as demonstrated by both early filling percentage (EFP, Table 2) and by the ratio of early to late ventricular filling velocity (E/A ratio). Both of these parameters have a strong linear correlation with age [EFP: $r = -0.72$, $P < 0.0001$ (Fig. 2*A*); E/A ratio: $r = -0.69$, $P < 0.0001$].

There was a significant correlation between age and the PCr/ATP ratio ($r = -0.52$, $P < 0.003$), with PCr/ATP reducing with age. This reduction in PCr/ATP was particularly pronounced in the older age group, since the PCr/ATP ratio was not significantly different between the young and middle-aged groups (Table 2 and Fig. 2*B*) but in the older group was significantly reduced: sample spectra are presented in Fig. 3. There was no correlation between the PCr/ATP ratio, LV mass, or LV mass index.

Cardiac torsion and strain. The relationship between LV torsion and strain was altered by aging. The peak LV torsion tended to increase with age, although not reaching significance (Table 2). Endocardial and whole wall circumferential strain decreased across the age groups, being significantly smaller in the oldest group compared with the youngest. With these effects working in opposite directions, the TSR increased

Table 1. *Morphology and blood pool measures*

	Age, yr			
	20–40	40–60	60+	ANOVA Significance
n	17	17	15	
Body mass index, kg/m^2	25.9 ± 5.5	27.7 ± 3.6	27.5 ± 2.9	
Weight, kg	74 ± 12	79 ± 12	82 ± 13	
Age, yr	30.5 ± 6.1	47.7 ± 5.7	62.3 ± 2.3	y/m[e], y/o[e], m/o[e]
Systolic blood pressure, mmHg	122 ± 10	128 ± 11	136 ± 14	y/o[d]
Diastolic blood pressure, mmHg	72 ± 8	82 ± 8	75 ± 8	y/m[d]
Heart rate, beats/min	58 ± 11	62 ± 10	59 ± 11	
Left ventricular mass, g	107 ± 28	111 ± 22	114 ± 26	
Left ventricular mass index, g/m^2	62 ± 14	58 ± 8	60 ± 12	
End systolic volume, ml	63 ± 15	47 ± 10	59 ± 19	y/m[d]
End diastolic volume, ml	149 ± 29	122 ± 18	139 ± 31	y/m[c]
Stroke volume, ml	85 ± 16	75 ± 13	80 ± 16	
End systolic index, ml/m^2	36 ± 7	25 ± 4	32 ± 10	y/m[e], m/o[a]
End diastolic index, ml/m^2	85 ± 14	65 ± 7	74 ± 15	y/m[e]
Stroke index, ml/m^2	49 ± 8	40 ± 7	42 ± 8	y/m[d], y/o[a]
Cardiac output, l/min	4.9 ± 0.9	4.6 ± 0.8	4.6 ± 1.0	
Ejection fraction, %	58 ± 4	62 ± 6	58 ± 7	
Eccentricity ratio, g/ml	0.72 ± 0.14	0.92 ± 0.16	0.82 ± 0.11	y/m[d]
Wall thickness systole, mm	10.0 ± 1.5	11.4 ± 2.2	11.7 ± 1.7	y/o[a]
Wall thickness diastole, mm	6.4 ± 1.1	7.2 ± 1.4	7.2 ± 0.9	
Arterial elastance	2.31 ± 0.39	2.99 ± 0.70	2.99 ± 0.42	y/m[d], y/o[d]
Ventricular elastance	3.25 ± 0.82	4.81 ± 0.91	4.23 ± 1.64	y/m[c]
Ventricular-arterial coupling	0.73 ± 0.13	0.63 ± 0.15	0.77 ± 0.20	

Values are means ± SD; *n*, no. of subjects. The ANOVA significance table shows which groups differ from each other with statistical significance following ANOVA testing with Bonferroni post hoc correction. The *P* values listed refer to the post hoc analysis. y, young; m, middle; o, old. [a]$P < 0.05$, [c]$P < 0.001$, [d]$P < 0.006$, and [e]$P < 0.0005$.

significantly with aging ($r = 0.44$, $P < 0.02$, Fig. 2*C*). This change with aging, like the alteration of cardiac energetics, was only significant in the older age group (Table 2).

Previous studies have demonstrated a decline in the rate of torsion release with increasing age (25). Our data did not demonstrate a significant difference between groups of the torsion recoil rate, which normalizes torsion measurements through the cardiac cycle by the maximum torsion achieved, eliminating the effect of different peak torsions between groups (Table 2). Neither was there significant change with aging in the residual torsion at 150% of the end-systolic time. There was no correlation between recoil rate (which is normalized for peak torsion) in diastole and EFP.

There was no significant difference in longitudinal shortening or radial thickening between the age groups, although there was a trend for reduced longitudinal shortening and increased radial thickening with aging that did not reach statistical significance. Wall thickness at systole increased progressively between the age groups but was only significantly different between the young and old groups (Table 2).

Correlations between modalities. By simple Pearson correlation between the three most significant variable results (PCr/ATP ratio, TSR, and EFP, Table 3), TSR negatively correlated very strongly with EFP ($r = -0.63$, $P < 0.0001$) while there was no significant correlation between EFP and the PCr/ATP ratio [$r = 0.34$, not significant (NS)] or between the PCr/ATP ratio and TSR ($r = -0.30$, P = NS). If we compare the variance in TSR explained by age and EFP, EFP determined more of the variance in TSR than age.

Changes in TSR, energetics, and EFP compared with determinants of global cardiovascular function. Potentially the three key parameters studied might be influenced by age directly but might be more strongly explained by the three major determinants of cardiovascular function: afterload (E_a), ventricular contractility (E_{es}), or preload (end-diastolic volume). Table 4 displays the results of the Pearson correlations. Age explained the greatest amount of variance in TSR. Age was the only parameter that could describe a significant amount of variance of the PCr/ATP ratio. Variation in the EFP could be accounted for most significantly by a change of age, but the change in arterial and ventricular elastance could describe a significant amount of the variance, with increased afterload and contractility being negatively associated with EFP (i.e., impaired early diastolic filling of the left ventricle). End-diastolic volume showed the weakest correlation with EFP.

Gender. There were no significant differences between any of the measured parameters based on gender.

DISCUSSION

This study has for the first time examined the effect of aging on the heart in subjects without cardiovascular disease or hypertension using the combined techniques of phosphorus spectroscopy to measure cardiac energetics, cardiac tagging to measure torsion and circumferential strain, and cine MRI to measure morphology. There are three principal age-related changes in the left ventricle: a decrease in PCr/ATP, impairment of global early diastolic function as characterized by the EFP, and an increase in the TSR indicating subendocardial dysfunction. Of these three parameters, EFP and TSR are strongly correlated with each other, although there is no significant relationship of these two variables with cardiac energetics, suggesting that the functional abnormalities do not have a major energetic basis. EFP also has a significant relationship to E_a and ventricular elastance, with higher age-related values of arterial and ventricular elastance associated with impairment of early filling in diastole.

It is well documented that, in normal aging without cardiovascular disease or hypertension, there is a decline in early diastolic function characterized by a prolongation of isovolumic relaxation time (τ) derived from the LV pressure waveform, reduction in the early diastolic filling rate, and augmentation of atrial contraction (3, 16, 31). The mechanism of this has been thought to be due to impaired LV relaxation (32), although this concept has been challenged more recently. Yamakado et al. (36) in a catheterization study were unable to demonstrate any age-related decline in the rate of LV pressure fall. Hees et al. (13) in a combined echocardiography and MRI study addressed the hypothesis that a decline in diastolic filling with age was more due to changes in early diastolic left atrial

Table 2. *Cardiac energetics, wall motion, and diastolic function measures*

	Age, yr			
	20–40	40–60	60+	ANOVA sig.
PCr/ATP (−)	1.97 ± 0.17	1.91 ± 0.15	1.73 ± 0.17	y/o[d], m/o[b]
Torsion-to-shortening ratio, rad	0.43 ± 0.13	0.48 ± 0.11	0.62 ± 0.18	y/o[c], m/o[a]
Peak torsion, deg	5.8 ± 1.8	6.3 ± 1.4	7.2 ± 1.6	
Peak whole wall circumferential strain, %	19.5 ± 3.7	18.0 ± 2.4	16.8 ± 2.8	y/o[a]
Peak endocardial circumferential strain, %	23.8 ± 4.0	23.1 ± 2.7	21.1 ± 3.9	
Torsion recoil rate, %/ms	0.30 ± 0.19	0.31 ± 0.11	0.23 ± 0.12	
Maximum torsion gradient in diastole, deg/ms	0.022 ± 0.013	0.027 ± 0.011	0.024 ± 0.011	
Residual torsion at 150% end-systolic time, deg	2.3 ± 1.8	2.2 ± 0.9	3.2 ± 2.0	
Longitudinal shortening, %	18.4 ± 2.3	17.3 ± 3.9	16.7 ± 2.1	
Radial thickening, %	58 ± 21	59 ± 13	64 ± 20	
Early filling percentage, %	80 ± 7	70 ± 7	63 ± 8	y/m[c], y/o[e], m/o[a]
E/A ratio	3.4 ± 1.7	1.7 ± 0.6	1.2 ± 0.5	y/m[e], y/o[e]
Early diastolic filling rate, ml/s	424 ± 143	369 ± 84	284 ± 71	y/o[d]
Late diastolic filling rate, ml/s	143 ± 53	235 ± 66	265 ± 80	y/m[c],y/o[e]
Deceleration time from early filling, ms	133 ± 32	118 ± 32	182 ± 66	y/o[a], m/o[d]

Values are means ± SD. The ANOVA significance table shows which groups differ from each other with statistical significance following ANOVA testing with Bonferroni post hoc correction. PCr/ATP, phosphocreatine-to-ATP ratio; rad, radians; E/A ratio, ratio of early to late ventricular filling velocity. The P values listed refer to the post hoc analysis. [a]$P < 0.05$, [b]$P < 0.02$, [c]$P < 0.006$, [d]$P < 0.001$, and [e]$P < 0.0005$.

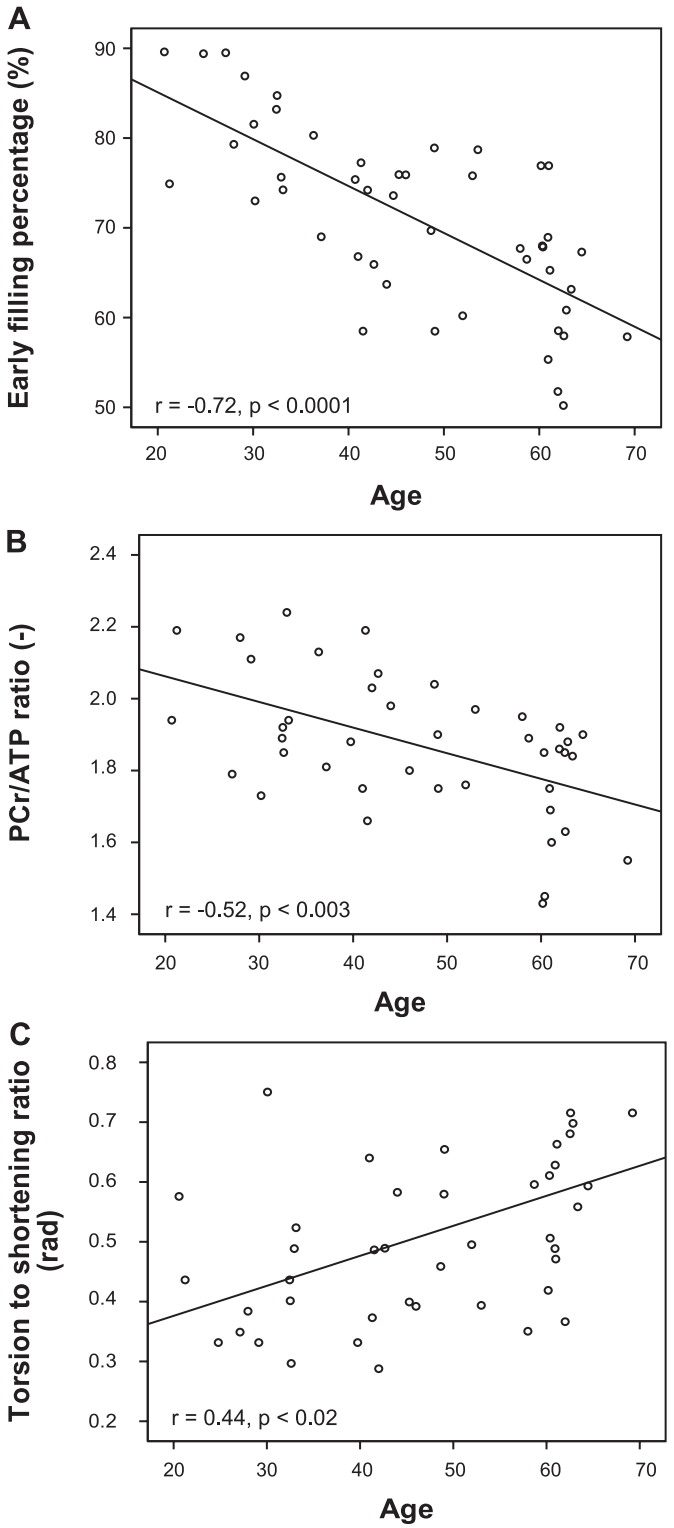

Fig. 2. Key cardiac parameters plotted against subject age. *A*: early filling percentage, representing the percentage of stroke volume due to ventricular relaxation. *B*: cardiac energetics represented by the ratio of phosphocreatine to ATP (PCr/ATP ratio). *C*: cardiac wall motion represented by the torsion-to-shortening ratio. rad, Radians.

pressure than LV relaxation. LV filling is determined by the atrioventricular pressure gradient, dependent on LV pressure decline and left atrial pressure. Using Doppler measures of early diastolic left atrial pressures, they demonstrated that the reduced age-related early diastolic filling was significantly related to these, but not measures of LV relaxation. One MR measure of LV relaxation is the torsion recoil rate in diastole, which has been shown to closely correlate with τ (10). Our data also show that there is no effect of aging on torsion recoil rates, in keeping with these data.

Our data also show a significant relationship of EFP with the TSR, so that as TSR increases, there is a decline in early filling. The TSR is a measure of subepicardial torsion exerting its mechanical advantage over the subendocardium, forcing the subendocardium to contract in the direction of the subepicardial fiber orientation (19). This can be well demonstrated in studies looking at human torsion that have a very high temporal resolution. For instance, in human heart transplant recipients who have had radio-opaque markers implanted at the time of transplant, torsion can be tracked with fluoroscopy throughout the cardiac cycle (12). The subendocardium normally contracts first in early systole as the specialized conducting fibers depolarize there before the subepicardium. Thus, in very early systole, the heart twists in a clockwise direction (when viewed from apex to base) for a short period of time when the subendocardial fibers are allowed to contract without influence

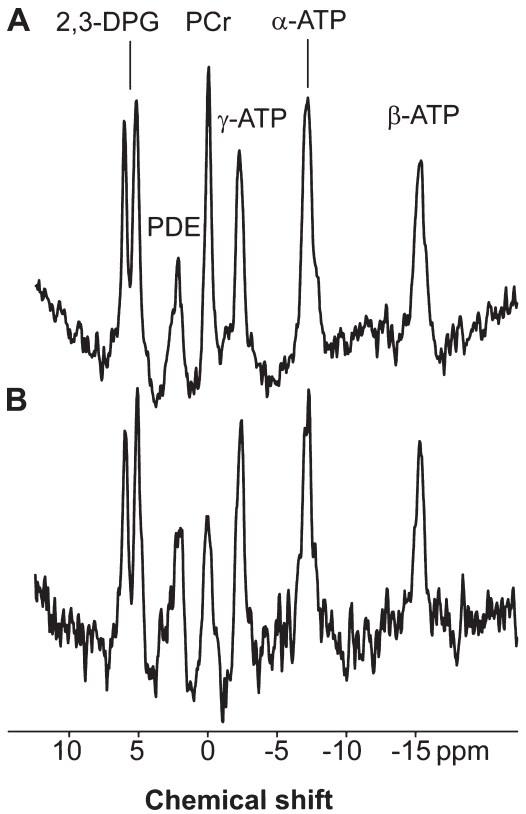

Fig. 3. Sample cardiac phosphorus spectra from a young subject (with PCr/ATP = 1.95, *A*) and an older subject (with PCr/ATP = 1.55, *B*). A difference in PCr concentration is seen. The spectra are presented as acquired before correction for saturation due to heart rate, flip angle experienced at the cardiac tissue, and blood content. 2,3-DPG, 2,3-diphosphoglycerate; ppm, parts/million; PDE, phosphodiesters.

Table 3. *Correlations between three principal age-related changes in left ventricular function and energetic (P values corrected for multiple comparisons)*

Outcome Measure	Pearson Correlation With:	r	P
Torsion-to-shortening ratio	Age	0.44	0.02
	Early filling percentage	−0.63	<0.0001
	PCr/ATP	−0.30	0.6
Early filling percentage	Age	−0.72	<0.0001
	Torsion to shortening ratio	−0.63	<0.0001
	PCr/ATP	0.34	0.2
PCr/ATP ratio	Age	−0.52	<0.003
	Early filling percentage	0.34	0.2
	Torsion to shortening ratio	−0.30	0.6

from the subepicardium. As soon as the subepicardium starts to contract, counterclockwise torsion develops. TSR has been shown to increase with aging, and this relative subendocardial dysfunction has been postulated to be due to subendocardial fibrosis (19). Subendocardial dysfunction should logically lead to a proportionate reduction in longitudinal shortening, due to the subendocardial fiber direction, as shown in hypertrophic cardiomyopathy (26): our data show a consistent trend for reduced longitudinal shortening with increasing age to accompany the rise in TSR (Table 2), although this does not reach statistical significance with this number of subjects.

That our data show that EFP is also significantly negatively related to E_a and ventricular elastance is also consistent with the above statements. It is known that vascular stiffness increases in normal human aging (34). Ventricular elastance is used as a load-independent marker of LV contractility (30). However, in the context of aging, ventricular elastance can increase, which may reflect more an increase in systolic stiffness of the ventricle as opposed to being a measure of the contractile state of the heart. Kawaguchi et al. (15) have shown using pressure-volume loop studies in human subjects with heart failure and normal ejection fractions that there was evidence of diastolic dysfunction as expected. However, there was an increase in E_a due to reduced arterial compliance, and this closely correlated with increased ventricular elastance, although it was not possible to determine whether systolic stiffness of the ventricle or higher contractility underpinned the change in E_{es}. The authors concluded that patients with heart failure with normal ejection fractions have systolic-ventricular and arterial stiffening beyond that associated with aging and/or hypertension. In a mouse model of muscular dystrophy cardiomyopathy that develops marked LV fibrosis in response to steroids, there is also an increase in ventricular elastance that is related to the extent of histological fibrosis (2). These data are entirely in keeping with our data in normal subjects with early diastolic dysfunction and ventricular and arterial stiffening, albeit in significantly less advanced disease.

Whereas we know that afterload can cause relaxation abnormalities in experimental models (5), and we demonstrate a significant relationship between EFP and E_a, we did not find a significant effect of aging on measures of LV diastolic torsion recoil. Age-related increases in afterload could affect early diastolic function by altering LV pressure relaxation, which as stated above can be measured by diastolic torsion recoil (10). Alternatively, a unifying hypothesis is one of left atrial, ventricular, and vascular stiffening. This systemic phenomenon causes an increase in the TSR, since the subendocardium is preferentially affected, and an increase in E_a due to vascular stiffness. EFP is reduced due to a fall in left atrial pressures. Hees et al. (13) have hypothesized that this is due to the aging left atrium becoming both flaccid at low volumes although stiff due to endocardial fibrosis at high volumes. At low volumes, the left atrial pressure might be low due to flaccidity, but at high volumes the pressure might be high due to increased stiffness.

Whereas there was a significant fall in the PCr/ATP ratio with age, the PCr/ATP ratio had no significant relationship with the other two major functional changes with age, TSR and EFP. Whereas cardiac contraction is an energy-consuming process, these data suggest that the age-related changes in diastolic and systolic function do not have a major energetic basis, and so is consistent with the hypothesis of age-related

Table 4. *Changes in TSR, energetics, and EFP compared with determinants of global cardiovascular function (P values corrected for multiple comparisons)*

Outcome Measure	Pearson Correlation With:	r	P
Torsion-to-shortening ratio	Age	0.44	0.04
	E_a	0.29	0.1
	E_{es}	0.39	0.24
	End diastolic volume	−0.27	0.96
PCr/ATP ratio	Age	−0.52	<0.005
	E_a	−0.21	1
	E_{es}	−0.14	1
	End diastolic volume	0.18	1
Early filling percentage	Age	−0.72	< 0.0001
	E_a	−0.57	< 0.0001
	E_{es}	−0.48	< 0.02
	End diastolic volume	0.34	0.3

TSR, torsion-to-shortening ratio; EFP, early filling pressure; E_a, arterial elastance; E_{es}, ventricular elastance.

changes due to fibrosis and stiffening in the left atrium, left ventricle, and vasculature. Our results are in broad agreement with previous attempts to examine the effects of aging on cardiac energetics. Between the young and old groups, we found a decrease in the PCr/ATP ratio of 12%. This is similar to the 15% decrease found by Schocke et al. (29). These results are also in agreement with results by Okada et al. (24) and Köstler et al. (17) where the majority of subjects studied were below the age of 60 and where no change in the ratio of PCr/ATP was found, as found between the two younger groups in our study.

Limitations of this study include the fact that cardiac energetic measurements are not spatially localized to the same extent as imaging measures and are taken predominantly from the anterior cardiac wall, whereas cardiac morphology and tagging measures take into account the entire left ventricle mass. Our oldest subject was only 69 years old, and this may have prevented us seeing some of the most severe alterations in diastolic function, wall motion, and cardiac energetics possible in the oldest patients. Subject numbers were limited, and this led to underpowering on some variables, notably longitudinal shortening, which might have been found to significantly decrease with age with a larger cohort. The changes in end-diastolic and end-systolic volumes with age are not linear, with a reduction in the middle-aged group. This has not been seen in other studies (8, 18), and the reason for this is unclear and is not explained by our data.

In conclusion, normal aging of the left ventricle is characterized by impaired early diastolic filling, an increase in the TSR, and reduced cardiac energetics. Whereas the functional measures are closely related, they do not have a major energetic component. This understanding of normal aging of the heart provides important information necessary to understand age-related cardiovascular diseases such as diastolic heart failure.

ACKNOWLEDGMENTS

We thank the patients and volunteers for contributing to this study. In addition, we acknowledge the significant contribution from Lilian Fairbairn-Smith and Judith Coulson, Research Nurses, and Tim Hodgson, Tamsin Gaudie, Carol Smith, and Louise Morris, the Research Radiographers.

K. G. Hollingsworth designed the experiments, analyzed and interpreted the data, contributed to the first draft of the manuscript along with G. A. MacGowan and subsequently revised it. A. M. Blamire, B. D. Keavney, and G. A. MacGowan were involved in the interpretation of the data, the drafting of the manuscript and its revision.

GRANTS

The study was funded by the Newcastle NIHR Biomedical Research Centre in Ageing (Stroke and Cardiovascular theme).

DISCLOSURES

No conflicts of interest are declared by the authors.

REFERENCES

1. **Arts T, Reneman RS, Veenstra PC.** A model of the mechanics of the left-ventricle. *Ann Biomed Eng* 7: 299–318, 1979.
2. **Bauer R, MacGowan GA, Blain A, Bushby K, Straub V.** Steroid treatment causes deterioration of myocardial function in the delta-sarcoglycan-deficient mouse model for dilated cardiomyopathy. *Cardiovasc Res* 79: 652–661, 2008.
3. **Benjamin EJ, Levy D, Anderson KM, Wolf PA, Plehn JF, Evans JC, Comai K, Fuller DL, Sutton MS.** Determinants of Doppler indexes of left-ventricular diastolic function in normal subjects (The Framingham Heart-Study). *Am J Cardiol* 70: 508–515, 1992.
4. **Borlaug BA, Melenovsky V, Redfield MM, Kessler K, Chang HJ, Abraham TP, Kass DA.** Impact of arterial load and loading sequence on left ventricular tissue velocities in humans. *J Am Coll Cardiol* 50: 1570–1577, 2007.
5. **Brutsaert DL, Declerck NM, Goethals MA, Housmans PR.** Relaxation of ventricular cardiac-muscle. *J Physiol* 283: 469–480, 1978.
6. **Buchalter MB, Weiss JL, Rogers WJ, Zerhouni EA, Weisfeldt ML, Beyar R, Shapiro EP.** Noninvasive quantification of left-ventricular rotational deformation in normal humans using magnetic-resonance-imaging myocardial tagging. *Circulation* 81: 1236–1244, 1990.
7. **Buchli R, Boesiger P.** Comparison of methods for the determination of absolute metabolite concentrations in human muscles by P-31 MRS. *Magn Reson Med* 30: 552–558, 1993.
8. **Cheng S, Fernandes VRS, Bluemke DA, McClelland RL, Kronmal RA, Lima JAC.** Age-related left ventricular remodeling and associated risk for cardiovascular outcomes: the multi-ethnic study of atherosclerosis. *Circ Cardiovasc Imaging* 2: 191–198, 2009.
9. **Conway MA, Bottomley PA, Ouwerkerk R, Radda GK, Rajagopalan B.** Mitral regurgitation: impaired systolic function, eccentric hypertrophy, and increased severity are linked to lower phosphocreatine/ATP ratios in humans. *Circulation* 97: 1716–1723, 1998.
10. **Dong SJ, Hees PS, Siu CO, Weiss JL, Shapiro EP.** MRI assessment of LV relaxation by untwisting rate: a new isovolumic phase measure of tau. *Am J Physiol Heart Circ Physiol* 281: H2002–H2009, 2001.
11. **Haase A, Hanicke W, Frahm J.** The influence of experimental parameters in surface-coil NMR. *J Magn Reson* 56: 401–412, 1984.
12. **Hansen DE, Daughters GT, Alderman EL, Ingels NB, Stinson EB, Miller DC.** Effect of volume loading, pressure loading, and inotropic stimulation on left-ventricular torsion in humans. *Circulation* 83: 1315–1326, 1991.
13. **Hees PS, Fleg JL, Dong SJ, Shapiro EP.** MRI and echocardiographic assessment of the diastolic dysfunction of normal aging: altered LV pressure decline or load? *Am J Physiol Heart Circ Physiol* 286: H782–H788, 2004.
14. **Jones DEJ, Hollingsworth K, Fattakhova G, MacGowan G, Taylor R, Blamire A, Newton JL.** Impaired cardiovascular function in primary biliary cirrhosis. *Am J Physiol Gastrointest Liver Physiol* 298: G764–G773, 2010.
15. **Kawaguchi M, Hay I, Fetics B, Kass DA.** Combined ventricular systolic and arterial stiffening in patients with heart failure and preserved ejection fraction - Implications for systolic and diastolic reserve limitations. *Circulation* 107: 714–720, 2003.
16. **Kitzman DW, Sheikh KH, Beere PA, Philips JL, Higginbotham MB.** Age-related alterations of Doppler left-ventricular filling indexes in normal subjects are independent of left-ventricular mass, heart-rate, contractility and loading conditions. *J Am Coll Cardiol* 18: 1243–1250, 1991.
17. **Köstler H, Landschutz W, Koeppe S, Seyfarth T, Lipke C, Sandstede J, Spindler M, von Kienlin M, Hahn D, Beer M.** Age and gender dependence of human cardiac phosphorus metabolites determined by SLOOP P-31 MR spectroscopy. *Magn Reson Med* 56: 907–911, 2006.
18. **Lakatta EG, Levy D.** Arterial and cardiac aging: major shareholders in cardiovascular disease enterprises. Part II. The aging heart in health: Links to heart disease. *Circulation* 107: 346–354, 2003.
19. **Lumens J, Delhaas T, Arts T, Cowan BR, Young AA.** Impaired subendocardial contractile myofiber function in asymptomatic aged humans, as detected using MRI. *Am J Physiol Heart Circ Physiol* 291: H1573–H1579, 2006.
20. **MacGowan GA, Koretsky AP.** Inotropic and energetic effects of altering the force-calcium relationship: mechanisms, experimental results, and potential molecular targets. *J Card Fail* 6: 144–156, 2000.
21. **Maslov MY, Chacko VP, Stuber M, Moens AL, Kass DA, Champion HC, Weiss RG.** Altered high-energy phosphate metabolism predicts contractile dysfunction and subsequent ventricular remodeling in pressure-overload hypertrophy mice. *Am J Physiol Heart Circ Physiol* 292: H387–H391, 2007.
22. **Neubauer S.** Mechanisms of disease: the failing heart: an engine out of fuel. *N Engl J Med* 356: 1140–1151, 2007.
23. **Neubauer S, Horn M, Cramer M, Harre K, Newell JB, Peters W, Pabst T, Ertl G, Hahn D, Ingwall JS, Kochsiek K.** Myocardial phosphocreatine-to-ATP ratio is a predictor of mortality in patients with dilated cardiomyopathy. *Circulation* 96: 2190–2196, 1997.
24. **Okada M, Mitsunami K, Inubushi T, Kinoshita M.** Influence of aging or left ventricular hypertrophy on the human heart: Contents of phospho-

rus metabolites measured by P-31 MRS. *Magn Reson Med* 39: 772–782, 1998.
25. **Oxenham HC, Young AA, Cowan BR, Gentles TL, Occleshaw CJ, Fonseca CG, Doughty RN, Sharpe N.** Age-related changes in myocardial relaxation using three-dimensional tagged magnetic resonance imaging. *J Cardiovasc Magn Res* 5: 421–430, 2003.
26. **Pasipoularides A.** LV twisting and untwisting in HCM: ejection begets filling Diastolic functional aspects of HCM. *Am Heart J* 162: 798–810, 2011.
27. **Rademakers FE, Rogers WJ, Guier WH, Hutchins GM, Siu CO, Weisfeldt ML, Weiss JL, Shapiro EP.** Relation of regional cross-fiber shortening to wall thickening in the intact heart: 3-dimensional strain analysis by NMR tagging. *Circulation* 89: 1174–1182, 1994.
28. **Schar M, Kozerke S, Fischer SE, Boesiger P.** Cardiac SSFP imaging at 3 tesla. *Magn Reson Med* 51: 799–806, 2004.
29. **Schocke MFH, Metzler B, Wolf C, Steinboeck P, Kremser C, Pachinger O, Jaschke W, Lukas P.** Impact of aging on cardiac high-energy phosphate metabolism determined by phosphorus-31 2-dimensional chemical shift imaging (31P 2D CSI). *Magn Reson Imaging* 21: 553–559, 2003.
30. **Suga H, Sagawa K.** Instantaneous pressure-volume relationships and their ratio in excised, supported canine left-ventricle. *Circ Res* 35: 117–134, 1974.
31. **Swinne CJ, Shapiro EP, Lima SD, Fleg JL.** Age-associated changes in left-ventricular diastolic performance during isometric-exercise in normal subjects. *Am J Cardiol* 69: 823–826, 1992.
32. **Tokushima T, Reid CL, Gardin JM.** Left ventricular diastolic function in the elderly. *Am J Geriatr Cardiol* 10: 20–29, 2001.
33. **Tyler DJ, Hudsmith LE, Clarke K, Neubauer S, Robson MD.** A comparison of cardiac P-31 MRS at 1.5 and 3 T Nmr. *Biomedicine* 21: 793–798, 2008.
34. **Vaitkevicius PV, Fleg JL, Engel JH, Oconnor FC, Wright JG, Lakatta LE, Yin FCP, Lakatta EG.** Effects of age and aerobic capacity on arterial stiffness in healthy-adults. *Circulation* 88: 1456–1462, 1993.
35. **Van der Toorn A, Barenbrug P, Snoep G, Van der Veen FH, Delhaas T, Prinzen FW, Maessen J, Arts T.** Transmural gradients of cardiac myofiber shortening in aortic valve stenosis patients using MRI tagging. *Am J Physiol Heart Circ Physiol* 283: H1609–H1615, 2002.
36. **Yamakado T, Takagi E, Okubo S, ImanakaYoshida K, Tarumi T, Nakamura M, Nakano T.** Effects of aging on left ventricular relaxation in humans: analysis of left ventricular isovolumic pressure decay. *Circulation* 95: 917–923, 1997.
37. **Zerhouni EA, Parish DM, Rogers WJ, Yang A, Shapiro EP.** Human heart tagging with MR imaging: a method for nonivasive assessment of myocardial motion. *Radiology* 169: 59–63, 1988.